



## BUILDING RESPONSE TO LONG-DISTANCE MAJOR EARTHQUAKES

**T.-C. PAN<sup>1</sup>, X. T. YOU<sup>2</sup> and K. W. CHENG<sup>3</sup>**

### SUMMARY

Singapore is believed to be located in an aseismic region. However, tremors caused by distant Sumatra earthquakes have reportedly been felt in Singapore for many years. Based on previous studies for Singapore, the maximum credible earthquakes (MCEs) from Sumatra have been hypothesized to be a subduction earthquake ( $M_w = 9.0$ ) and a strike-slip earthquake ( $M_w = 7.5$ ). Response at a soft soil site in Singapore to the synthetic bedrock motions corresponding to these maximum credible earthquakes are simulated using a one-dimensional wave propagation method based on the equivalent-linear technique. A typical high-rise residential building in Singapore is analyzed to study its responses subjected to the MCE ground motions at both the rock site and the soft soil site. The results show that the base shear force ratios would exceed the local code requirement on the notional horizontal load for buildings. Because of the large aspect ratio of the floor plan of the typical building, the effects of flexible diaphragms are also included in the seismic response analyses.

### INTRODUCTION

The 1985 Michoacan earthquake, in which a large earthquake ( $M_s = 8.1$ ) along the coast of Mexico, caused destructions and loss of lives in Mexico City, 350 km away from the epicenter. Learning from the Michoacan earthquake, it has been recognized that urban areas located rather distantly from earthquake sources may not be completely safe from the far-field effects of earth tremors. Singapore is located in a low-seismicity region, where the closest active seismic sources are located more than 300 km away, along and off the western coast of Sumatra. Earthquakes in Sumatra, some of which had magnitudes as low as 6.0, have frequently shaken high-rise buildings in Singapore, especially those founded on Quaternary marine clay deposits and reclaimed lands. No structural damage, however, has been recorded (Pan [1], Pan [2]). Although seismic hazard from such distant earthquakes, in terms of ground shaking, is considerably low, seismic risk, in terms of damage potential to structures, loss of lives and assets, cannot be ignored because of the high concentration of population and commercial activities taking place in structures that have not been designed specifically for seismic loads. Currently, building design codes for structures in Singapore and Malay Peninsula have been developed largely based on the BS8110 Code [3], which does not provide for seismic loadings.

<sup>1</sup> Professor and Director, Protective Technology Research Centre, School of Civil and Environmental Engineering, Nanyang Technological University, Singapore 639798. E-mail: tcpn@pmail.ntu.edu.sg

<sup>2</sup> Research scholar, School of CEE, NTU

<sup>3</sup> Research scholar, School of CEE, NTU

A recent study by Megawati [4] has identified the maximum credible earthquakes in Sumatra to be a subduction earthquake ( $M_w = 9.0$ ) off the west coast of Sumatra and a strike-slip earthquake ( $Mw = 7.5$ ) on the Great Sumatran Fault. Synthetic bedrock motions corresponding to the maximum credible Sumatra subduction earthquake and the strike-slip earthquake have been simulated (Megawati [4], Megawati [5], Pan [6]). A previous similar study by Pan [7] has considered site response at a soft soil site for a recorded Sumatra subduction earthquake ( $Mw = 7.0$ , epicentral distance = 540 km). This study considers site response at the same site to the synthetically generated maximum credible earthquake ground motions using the one-dimensional wave propagation method based on the equivalent-linear technique. The paper starts with a brief description of the seismotectonics of Sumatra and the geological formation of Singapore. The geotechnical properties of the soft soil site are then described which is followed by the procedure of the soil site response analysis. Finally, response spectrum analyses are carried out to study the seismic response of a typical high-rise residential building subjected to the maximum credible earthquakes.

## MAXIMUM CREDIBLE GROUND MOTIONS

### Seismotectonics of Sumatra

Sumatra is located adjacent to the Sunda trench (Figure 1), where the Indian-Australian plate subducts beneath the Eurasian plate at a rate of  $67 \pm 7$  mm per year towards  $N11^\circ E \pm 4^\circ$  (Tregoning [8]). The islands of Sumatra and Java lie on the over-riding plate, a few hundred kilometers from the trench. Convergence is nearly orthogonal to the trench axis near Java, but it is highly oblique near Sumatra, where the strain is strongly partitioned between dip slip on the subduction zone interface and right-lateral slip on the Sumatran fault along the western coast of the island. The earthquake focal mechanisms and the hypocentral distributions indicate that the subducting plate dips less than  $15^\circ$  beneath the outer arc ridge, and the dip angle becomes steeper to about  $50^\circ$  below the volcanic arc. The relatively shallow dip angle gives strong coupling between the over-riding and the subducting plates. As such, large earthquakes have been generated in the region. The largest subduction earthquake that has occurred in the Sunda trench is the great 1833 event with an estimated  $M_w$  magnitude between 8.8 and 9.2 (Zachariasen [9]). It was estimated to have caused a long rupture which measured more than 400 km between Enggano and Batu islands (Figure 1). Singapore is located almost perpendicular at an epicentral distance of 723 km to the centre of the rupture zone of 650 km (Figure 1). The earthquake, with an average  $M_w$  magnitude of 9.0, is selected to be the maximum credible earthquake that the Sumatra subduction zone is capable of generating (Megawati [4]).

The Sumatran fault lies roughly 250 km northeast of the trench. Geologic and geophysical evidences identify the fault as a seismically active right-lateral, strike-slip fault. The fault is a trench-parallel fault system, whose basic kinematic role is to accommodate a significant amount of the strike-slip component of the oblique convergence between the Indian-Australian plate and the Eurasian plate southwest to Sumatra. The 1650 km long fault runs along the western side of the Sumatra Island, coinciding with the Bukit Barisan mountain chain. The overall shape of the fault is sinusoidal, with the northern half of the fault concave to the southwest and the southern half of the fault concave to the northeast. The Sumatran fault is highly segmented, composing of 19 major segments with cross-strike width of step-overs between adjacent segments of about 5 to 12 km. The lengths of the segments range from 30 to 220 km. Due to the fact that the fault is highly segmented, it has a limited capacity to generate very large earthquakes. However, the fault is located relatively close to Singapore than the subduction zone. Historical records show that the segments of the Sumatran fault have caused numerous major earthquakes but their magnitudes are limited to about  $7.5 - 7.7$  with rupture lengths not greater than 100 km (Sieh [10]). Of the 19 segments of which the Sumatran fault is composed, the Suliti segment ( $1.75 - 1.0^\circ S$ , length  $\approx 95$  km), the Sumani segment ( $1.0 - 0.5^\circ S$ , length  $\approx 60$  km) and the Sianok segment ( $0.7^\circ S - 0.1^\circ N$ , length  $\approx 90$

km) are the closest segments to Singapore (Figure 1). Two major earthquakes have occurred in these segments. The first was on 4 Aug 1926 ( $M_s \approx 7.0$ ) and the second was on 9 June 1943 ( $M_s = 7.4-7.6$ ). Judging from the historical earthquake records and the geometrical segmentation of the Sumatran fault, the maximum credible earthquake that can be generated by the fault is a right-lateral event with a magnitude of  $M_w = 7.5$  in the Sumani segment (Megawati [4], Megawati [5], Pan [6]).

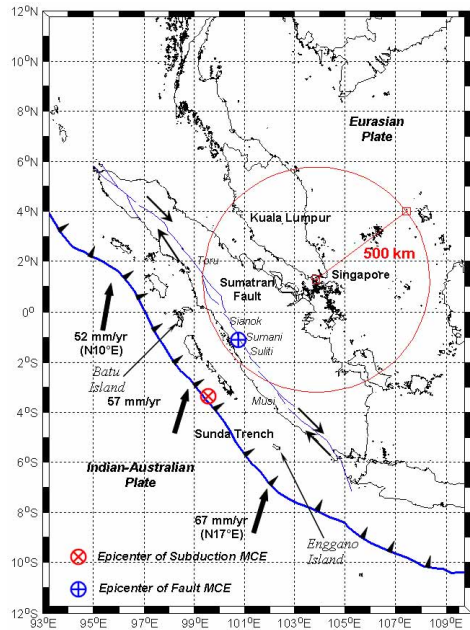


**Figure 1 The Sumatran Fault and the Sunda Trench with epicenters of the maximum credible earthquakes**

### Subsurface Soil Properties of the Site

The soft soil site is located at Katong Park (KAP) along the south-east coast of Singapore island (Figure 2). The site rests on the Kallang Formation which consists of late Pleistocene and recent deposits of marine, alluvial, littoral and estuarine origin. The most important unit of the Kallang Formation is the marine clay. It occurs over an area covering one quarter of the island, but no surface outcrops exist. Its thickness is extremely variable with a maximum recorded of 35 m (Pitts [11]). The marine clay is pale grey to dark blue in colour, soft, silty, kaolinite-rich and has shell fragments disseminated throughout.

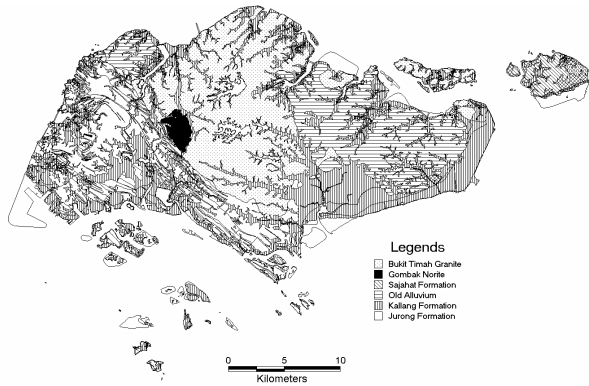


**Figure 2 Singapore surfacial geological map and location of the KAP site**

The subsurface profile of the KAP site and its shear-wave velocities are shown in Figure 3 and detailed descriptions of the soil layers are given in Table 1. It consists of 6.5 m of fill material, followed by 24 m of

marine clay unit. The marine clay unit consists of upper and lower members separated by a weathered crust on top of the lower member. This weathered crust is much stiffer than either the upper or the lower member, as can be deduced from the much larger recorded shear wave velocity. Following the marine unit is 4 m of soft organic clay, 5 m of residual soil and the last 8 m consists of slightly weathered silty sand of which the shear wave velocity reaches a maximum value of around 500 m/s.

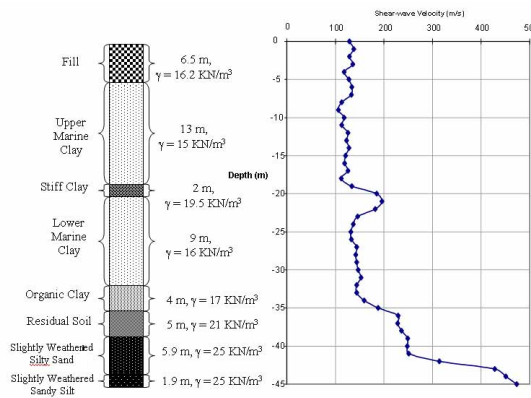


**Figure 3 Subsurface profile at the Katong Park (KAP) station**

**Table 1 Descriptions of subsurface soil materials at KAP**

Formation	Soil	Thickness (m)	Description
Fill	--	6.5	Man-made deposits of natural earth material consisting of loose clayey silt with some fine to coarse grain sand. Below -1.5m, material becomes loose sand. Colour is brownish-gray.
Alluvium	Upper Marine Clay	13	Very soft, high plasticity and high water content clay.
	Weathered Crust	2	Material is almost homogenous throughout with traces of seashells at -9.0m. Colour is blueish-gray.
	Lower Marine Clay	9	
	Organic Clay	4	
Old Alluvium	Residual Soil	5	Stiff to very stiff silty clay. Material is low in water content and clay has a moderate plasticity. Sample can be deformed by hand pressure.
	Slightly Weathered Silty Sand	5.9	Very dense silty sand with fine to coarse grain sand. Sample is stiff and cannot be deformed easily by fingers, but can be crushed into soil breccia
	Slightly Weathered Silt	1.9	Very stiff, friable silt that can be crushed into soil breccia

### The Maximum Credible Ground Motions

(Megawati [4], Megawati [5], Pan [6]) identified that the maximum credible ground motions in Singapore are likely to be caused by two large earthquakes of different source mechanisms. One is a strike-slip earthquake (Sumani segment) with an epicentral distance of around 425 km and a moment magnitude of 7.5. The other is a Sumatra subduction earthquake with an epicentral distance of 723 km and a moment magnitude of 9.0 (Figure 1). The bedrock motions in Singapore due to these two earthquakes have been simulated using the extended reflectivity method (Kohketsu [12]), taking into account uncertainties in the source rupture process. Detailed descriptions of the MCEs and the simulation process can be found in

separate publications (Megawati [4], Megawati [5], Pan [6]). One set of the simulated motions is used in this study. The three components of the strike-slip earthquake and the subduction earthquake are shown in Figures 4 and 5, respectively. The beginning of the signals corresponds approximately to the arrival in Singapore of the first p-waves from the sources. The directions of the tangential/radial components for the strike-slip earthquake and the parallel/perpendicular components for the subduction earthquake are defined in Figure 6. Response spectra (of 5% damping ratio) are shown in Figures 7 and 8, respectively, for the maximum credible earthquakes.

The larger of the two horizontal components of the synthetic MCE ground motions are thus used in the convolution process to obtain the surface accelerations at the soft soil site. They are the tangential acceleration component of the Sumatra strike-slip earthquake and the perpendicular acceleration component of the Sumatra subduction earthquake.

### Site Response Analysis

The borehole data of the KAP site provides the thickness, the average SPT N values and the shear wave velocity ( $V_s$ ) for each layer. The average bulk density and plasticity index PI for the soil layers are taken from a local study by Tan [13]. The shear wave velocity and the damping ratio for the elastic half-space are determined based on the results from Lee [14] for the Bukit Timah Granite. The value of  $G_{max}$  is determined from  $G_{max} = \rho V_s^2$ .

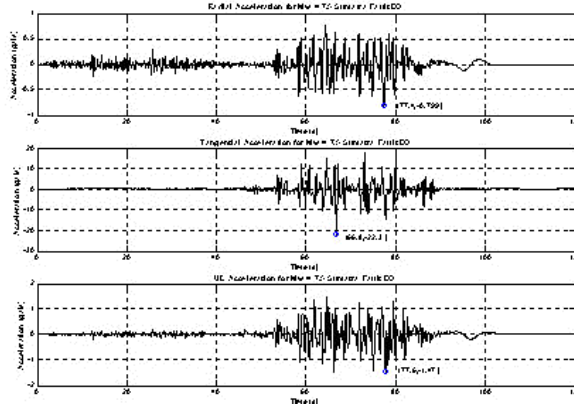


**Figure 4** Three acceleration components for the maximum credible strike-slip earthquake

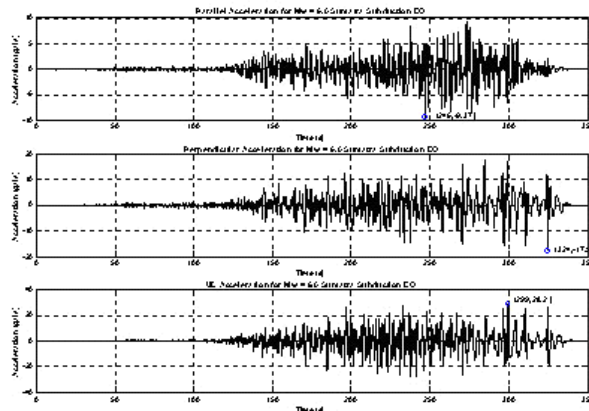


**Figure 5** Three acceleration components for the maximum credible Sumatra subduction earthquake

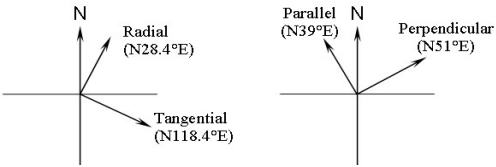


**Figure 6 Directions of the radial/tangential components for the strike-slip earthquake and parallel/perpendicular components for the subduction earthquake defined**

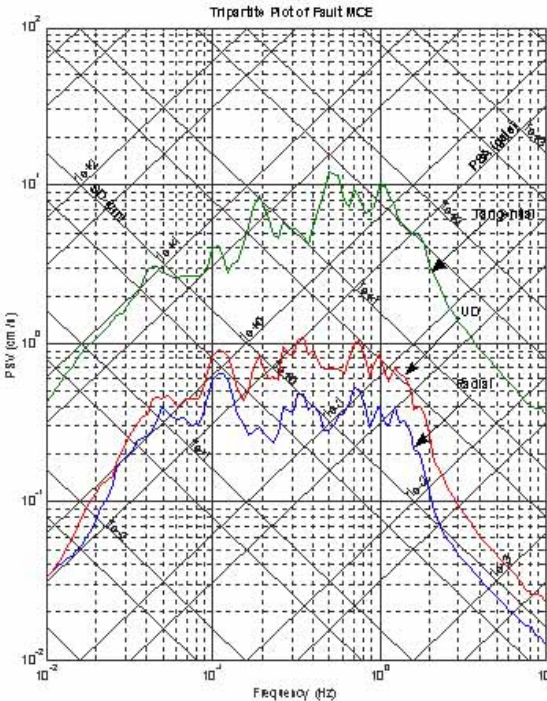


**Figure 7 Tripartite plot of response spectra (5% damping ratio) for the strike-slip MCE**

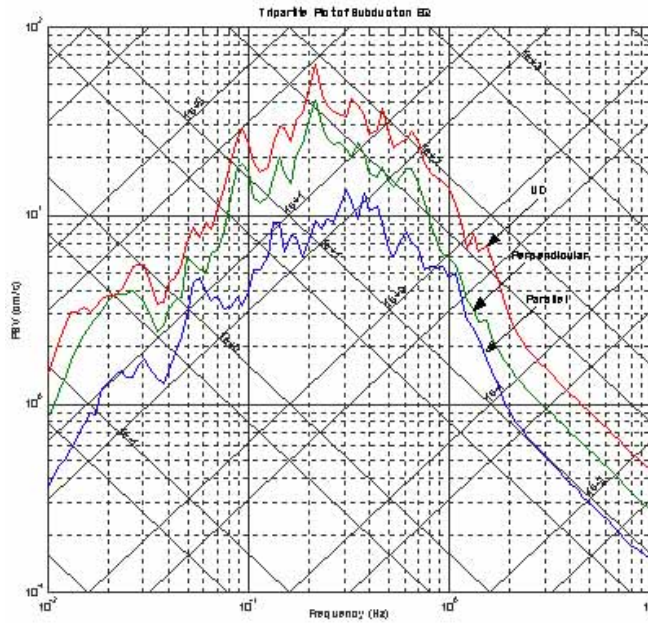


**Figure 8 Tripartite plot of response spectra (damping ratio = 5%) for the subduction MCE**

In the equivalent linear method, nonlinear behaviour of soil is accounted for by the use of strain-dependent stiffness and damping parameters. The stiffness of the soil is characterized by the maximum shear modulus  $G_{\max}$  and a modulus reduction curve, which shows how the shear modulus  $G$  decreases from  $G_{\max}$  at larger strains. Damping behaviour is characterized by the damping ratio, which increases with increasing strain amplitude. The current study uses the plasticity index to characterize both the  $G/G_{\max}$  and damping ratio curves for cohesive soils (Vucetic [15]). For cohesionless soils, the average  $G/G_{\max}$  and damping ratio curves developed by Seed [16] are used. The respective curves are shown in Figure 9 for soft clay ( $\text{PI} = 60$ ), stiff clay ( $\text{PI} = 30$ ) and sand ( $\text{PI} = 0$ ).

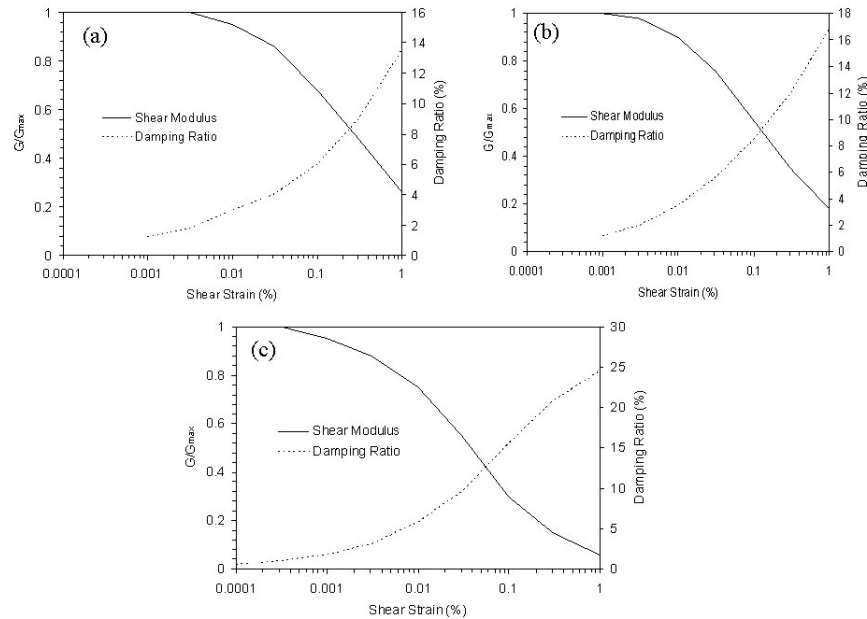


**Figure 9 Modulus reduction and damping ratio curves for (a) Soft Clay ( $\text{PI} = 60$ ), (b) Stiff Clay ( $\text{PI} = 30$ ) (after Vucetic [15]) and (c) Sand ( $\text{PI} = 0$ ) (after Seed [16])**

The equivalent linear site response analysis is carried out for the soft soil site using the two MCE ground motions described earlier. In this study, the EERA program (Bardet [17]) for equivalent-linear earthquake site response analysis of layered soil deposits, is used. The parameters used in EERA are summarized in Table 2. The simulated surface acceleration time-history and its Fourier and response spectra for the strike-slip tangential component are compared with those of the corresponding input rock motion (Figures 10 and 11). We observe an increase in the peak acceleration by around 2.2 times from 22.3 gals to 49.8 gals. In the Fourier domain, we notice a distinct predominant frequency at around 1.0 Hz for the surface motion as compared with the rock motion which does not display a distinct peak. Comparison between the surface and rock acceleration response spectra shows that amplification is observed to begin at around 0.2 or 0.3 Hz till the Nyquist frequency of 5.0 Hz. The peak spectral acceleration at the surface is about 240 gals (at around 1.0 Hz). Similar results for the subduction perpendicular components are shown in Figures 12 and 13. For the subduction event, we observe an increase in the peak acceleration by around 2.6 times from 17.5 gals to 45.6 gals (Figure 12). In the Fourier domain, we notice a distinct predominant frequency at around 0.8 Hz for the surface motion as compared with the rock motion which again does not display a distinct peak. Similar to the strike-slip event, comparison between the surface and rock acceleration response spectra shows that amplification begins at around 0.2 or 0.3 Hz till the Nyquist frequency of 5.0 Hz (Figure 13). The peak spectral acceleration at the surface is about 220 gals (at around 1.0 Hz).

The simulated transfer functions for both the strike-slip and the subduction events are depicted in Figure 14. We note that the site fundamental frequency is about 0.8 Hz. From the previous study by Pan [7] on the same site, the site fundamental frequency based on the recorded ground motions of a much weaker earthquake ( $M_w = 7.0$ , epicentral distance = 540 km) was found to be around 1.0 Hz. The difference in site fundamental frequency results from the much larger input motions used in this study, which induces more degradation in soil stiffness and consequently, a shift in the fundamental frequency towards a lower value.

**Table 2 Properties of Subsurface soil layers**

	Layer Number	Soil Material Type*	Thickness of layer (m)	Maximum shear modulus $G_{max}$ (MPa)	Total unit weight (kN/m <sup>3</sup> )	Shear wave velocity (m/sec)
Fill	1	(a)	6.5	24.04	16.38	120
Upp Marine Clay	2	(a)	13	23.18	15.79	120
Clay	3	(b)	2	70.03	19.03	190
Lower M Clay	4	(a)	9	35.53	16.58	145
Organic Clay	5	(b)	4	82	15.89	225
Residual soil	6	(b)	5	82	15.89	225
Silty Sand	7	(c)	5.9	104.81	20.31	225
Silt	8	(c)	1.9	408.51	20.7	440
Bedrock	9	-	-	19321.1	26	2700

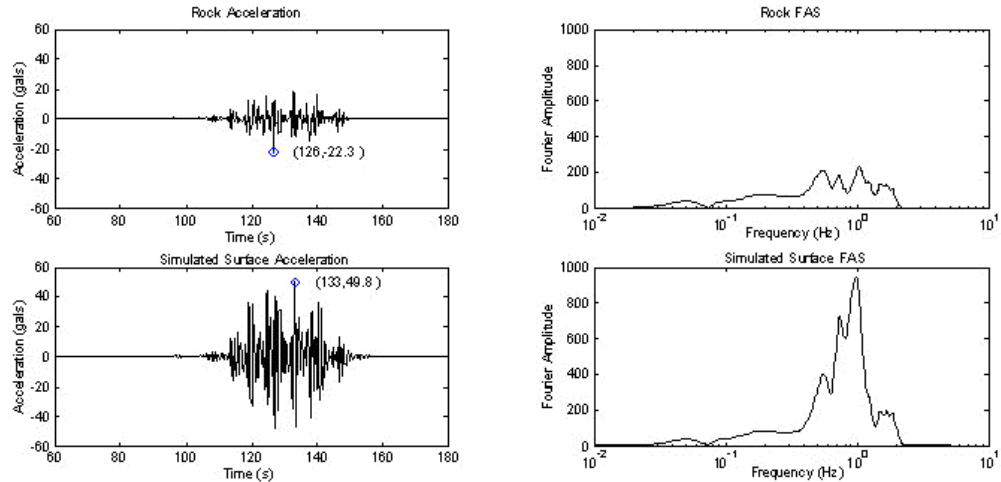


**Figure 10 Comparison of rock and surface acceleration time-histories and Fourier spectra for the  $M_w = 7.4$  Sumatra strike-slip earthquake**

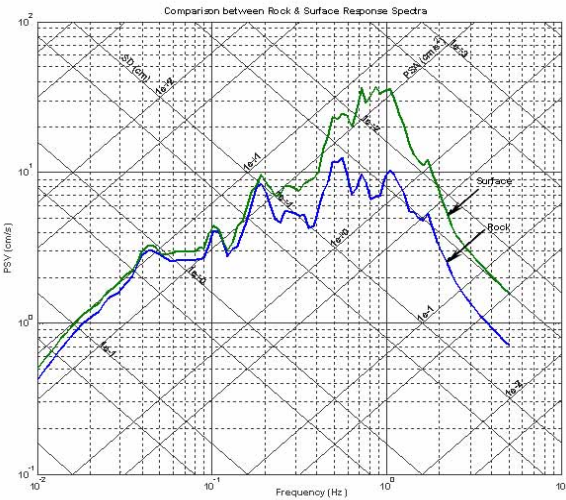


**Figure 11 Comparison of rock and surface response spectra for the Mw = 7.4 Sumatra strike-slip earthquake**

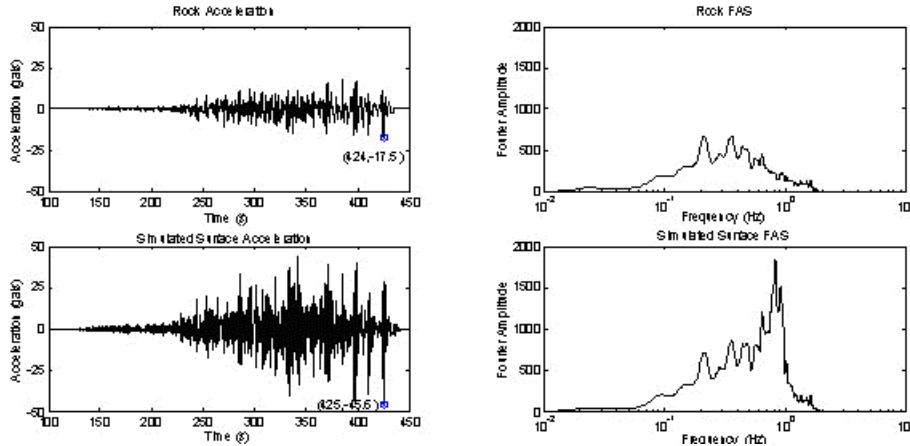


**Figure 12 Comparison of rock and surface acceleration time-histories and Fourier spectra for the Mw = 9.0 Sumatra subduction earthquake**

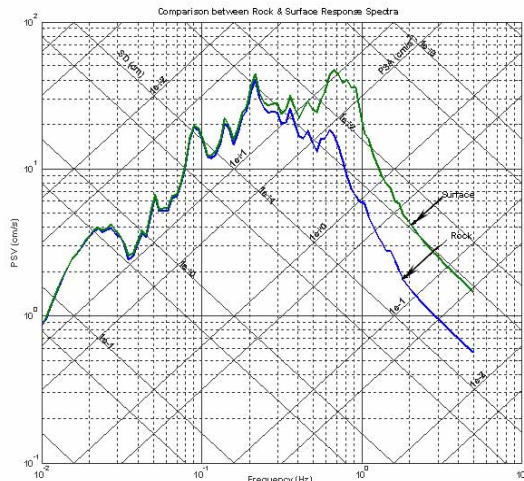


**Figure 13 Comparison of rock and surface response spectra for the Mw = 9.0 Sumatra subduction earthquake**

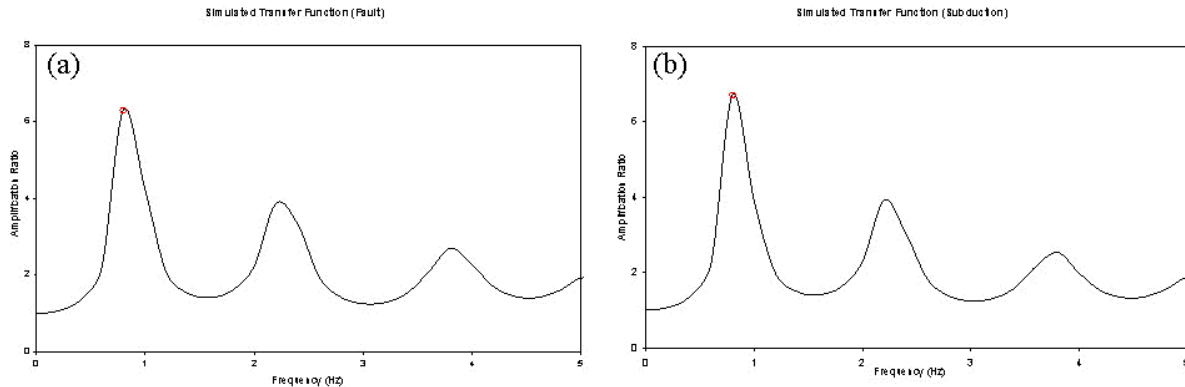


**Figure 14 Comparisons of transfer functions between (a) Sumatra strike-slip earthquake and (b) Sumatra subduction earthquake**

## BUILDING RESPONSE TO LONG-DISTANCE EARTHQUAKES

In this section, the responses of a typical high-rise residential building under the scenario earthquakes are studied. Both the rock and the soft soil site ground motions from the subduction and the strike-slip earthquakes described in the previous sections are used as the inputs. The responses to the different ground excitations are compared. Because of the unusual shape of the typical building, which will be further described later, the effects of flexible diaphragms are significant and thus, included in the finite element (FE) modeling.

### Building Descriptions

The structure under study is a typical 15-storey, reinforced concrete (RC) residential building. The overall height of the building is 42.8 m with the first storey of 3.6 m and the others 2.8 m. Figure 15 shows a typical floor plan of the building. The dimensions of the floor plan are 94.5 m in the longitudinal direction and 11 m in the transverse direction. The building has a reinforced concrete frame-shear wall dual structural system. No clear symmetry can be observed from the building drawings. The frame system consists of a series of two-bay frames spanning in the transverse direction. The frames are spaced at about 3 m along the longitudinal direction. The typical column sections are 0.3 m by 1.2 m for the first three stories, and 0.3 m by 0.9 m for the upper stories with the larger dimension along the transverse direction. Such wall-like columns are prohibited from the modern seismic design codes. The design provision for seismic loadings in ACI-318 [18] requires a minimum width to length ratio of 0.4. Thomas [19] reported severe damages of the wall-like columns in the Adana-Ceyhan earthquake of June 27, 1998. The typical beam size is 0.3 m by 0.5 m. Figure 16 shows the typical beam-column joint details. The wall system is made up with the three staircases located in the two ends and the middle of the building. The thickness of the wall panels is 0.2 m. The walls are also aligned mainly along the transverse direction. Therefore, the longitudinal direction appears to be the weaker direction. The partition walls inside the frames are made of bricks. The building holds eight units of flats, and the corridor is at one side of the building. The partition walls along the corridor are only half-high because of the large openings for the windows. The ground floor is an open area reserved for public usage. The floors are cast-in-situ reinforced concrete slabs with 0.125 m thickness. Because of the large aspect ratio of the floor dimensions, the effects of flexible diaphragms may be significant on the building's seismic response.

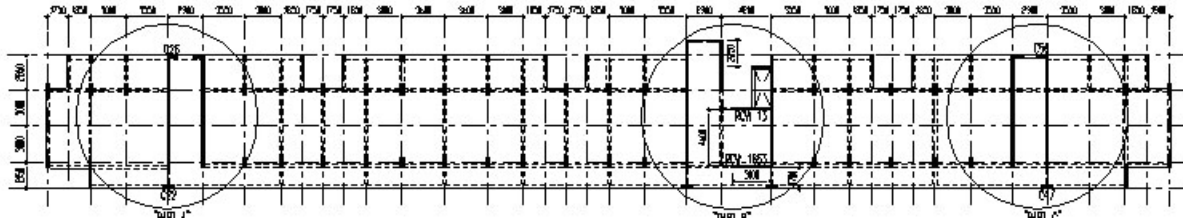


**Figure 15 The floor plan of the typical building**

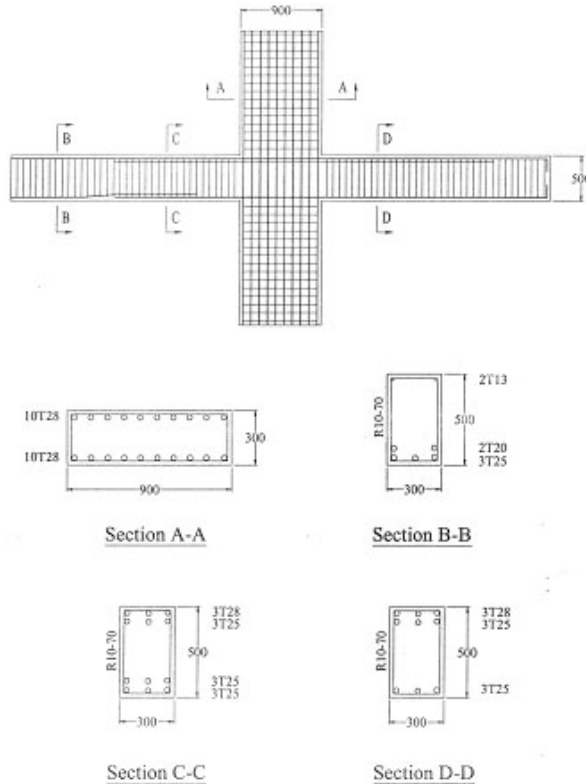


**Figure 16 The typical beam-column joint details**

### Finite Element Model

A three-dimensional (3D) FE model was constructed to study the dynamic characteristics of the building. The perspective view of the model is shown in Figure 17. In the model, the flexible floors were modeled using the shell elements, and the brick partition walls were included via the plane stress elements. Table 3 and Figure 18 show the first 4 modal frequencies and the mode shapes of the model, respectively. The fundamental frequency is 1.27 Hz in the transverse direction, which is contrast to the original expectation. This may be due to the brick infill walls which increase the stiffness in the longitudinal direction greatly. As shown, the first 3 modes of the model are primarily the global longitudinal or rotational modes, where the diaphragms behave rigidly. However, mode 4 is clearly a diaphragm deformation mode where the floors are bent as a flexible deep beam.

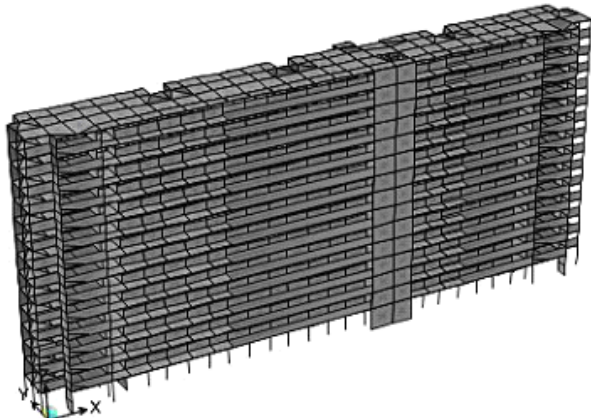


**Figure 17 The perspective view of the FE model**

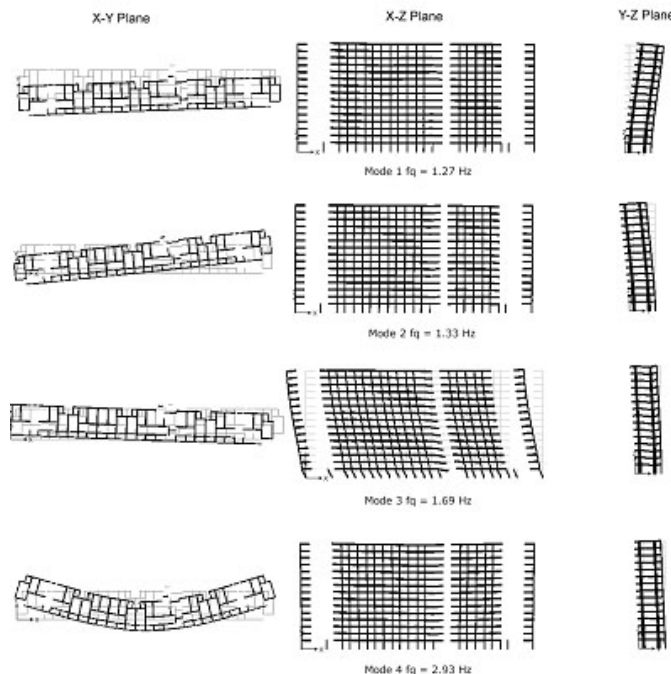


**Figure 18 The first 4 mode shapes of the FE model**

**Table 3 The first 4 natural frequencies of the model**

Mode	1	2	3	4
Freq. (Hz)	1.27	1.33	1.69	2.93

#### **Structural Response to Long-distance Earthquakes**

Two specific response spectra of the rock ground motions mentioned in the previous sections, one from the subduction perpendicular component and the other from the strike-slip tangential component, and their corresponding ground motions at a soft soil site are used as the inputs to the FE model. The ground motions are applied separately in the longitudinal and the transverse directions. The responses are summarized as follows.

### *Total Base Shear Forces*

The total base shear forces of the FE model subjected to the MCEs are shown in Tables 4 for both the longitudinal and the transverse directions. The maximum base shear force is 14056 kN, and caused by the soft soil ground motion of the strike-slip earthquake in the transverse direction. The force is about 9.2 % of the total building dead weight, which is 152563 kN. Even though the total base shear forces of the model are greater than 1.5% of the total building weight, which is the notional lateral resistant capacity required by BS8110 [3], they are all well below the base shear capacity of the building. The base shear capacities of the building are 22.4% and 35.3% of the building weight for the longitudinal and the transverse directions, respectively.

**Table 4 base shear forces of the building subjected to MCEs**

Earthquake	Soil Type	Longitudinal		Transverse	
		Shear Force (N)	Force/Weight (%)	Shear Force (N)	Force/Weight (%)
Strike-Slip	Rock	6014218	3.9%	5523890	3.6%
	Soil	13544143	8.9%	14055959	9.2%
Subduction	Rock	3771875	2.5%	4020698	2.6%
	Soil	9872679	6.5%	11020343	7.2%

### *Base Shear Forces of Individual Members*

The individual column shear capability of the building structure is studied via the ratios of the base shear forces of individual frames over their corresponding shear capacities. The ratios were calculated for the strike-slip earthquake case using its soft soil ground motions, because it can be seen from Table 4 that this ground motion generates the maximum total base shear forces. For both directions, all the ratios are below 70%. Therefore, the shear forces should not be a problem for individual frames during the MCE events.

### *Moment Response*

The moment responses of the vertical members were checked against their corresponding P-M-M interaction surfaces. It was found that when the building was loaded in the longitudinal direction, the moments in all the columns were below their capacities. However, when the building was loaded in the transverse direction, some columns were overstressed by the biaxial bending moments due to the shape of the building. It is very easy for a long-narrow building to have a rotational response, i.e. the forces applied in the transverse direction may generate a relatively significant response in the longitudinal direction.

### *Non-Structural Elements*

The brick partition walls play a very important role in the structural responses in this case: the direction of the fundamental mode is changed by including brick infills. The force demands of the brick walls during the MCE events are also compared with their capacities. The yielding capacity and the ultimate capacity of a typical brick panel are about 550 kN and 1800 kN, respectively. When the building is subjected to the bedrock motions of the MCEs, the forces taken by the brick panels are well below their yielding capacities. However, when the building is subjected to the soft soil motions of the MCEs in either of the longitudinal and transverse directions, the forces taken by some brick panels would fall between the yielding capacities and the ultimate capacities. Therefore, if the typical building is located at the soft soil sites, some cracks on the brick walls may be expected after the MCE events.

### *Site-Dependent Responses*

Table 4 shows that, when the ground motions change from the bedrock motions to the soft soil motions, the base shear forces are amplified by two to four times. For example, when the building is subjected to the bedrock motion of the strike-slip earthquake, the total base shear force is only 6014 kN, while when subjected to the soft soil motion of the same earthquake, the total base shear force increases to 13544 kN.

Therefore, the typical building would function very well during the MCE events when it is located at the rock sites. However, the MCE events might cause some damages to the building located at the soft soil site, such as overstressing on some column and cracking on the infill panels.

#### *Effects of Flexible Diaphragms*

It is believed that the building was designed under the assumption of rigid diaphragms in spite of the large aspect ratio of the floors, i.e. the lateral forces were distributed according to the stiffness of the vertical members. However, the building under study does experience the diaphragm deformation. Therefore, it is worthy to investigate how much the structural responses are different from the original design values. A sub-model was constructed by rigidly constraining all the floors of the existing FE model (Figure 17). The percentage changes of the base shear forces of the individual frames from the rigid model to the flexible model are calculated. It can be found that the maximum change in percentage is about 45% increase. The design force at this location calculated under the rigid diaphragm assumption would thus be underestimated. However, because the shear capacities of the columns designed under the gravity load are much larger than the shear force demands caused by the MCEs, the structure would still be safe in this case in terms of the shear forces. A more detailed study on the effects of flexible diaphragms can be found somewhere (Pan [20]).

## CONCLUSIONS

Ground motions at a soft soil site in Singapore due to the maximum credible earthquakes from Sumatra have been computed using a one-dimensional equivalent-linear ground response analysis technique. Due to the large input rock motions, soil stiffness degradation has been observed. This results in a consequent shift of the site fundamental frequency towards a lower value as compared with the linear case of the recorded weak earthquake motion. It has been shown that such maximum credible earthquakes are able to induce, at the soft soil site, spectral accelerations greater than 20 gals for a wide frequency range. The responses of a typical high-rise residential building subjected to the ground motions of MCEs were investigated. Even though the base shear forces caused by the earthquake ground motions would exceed the nominal code requirement stated in BS8110, the column members designed under the gravity loads are sufficient to resist them. The responses of the building are highly site-dependent. At the rock site, the earthquake ground motions are hardly a problem to the building. However, at a soft soil site, the MCEs may cause some columns being overstressed and cracking on the infill walls. Because of the large length/width aspect ratio of the building floors, the floor diaphragms behave flexibly. The flexibility of the diaphragms may increase the base shear force by 45% at certain locations.

## REFERENCES

1. Pan TC. "When the doorbell rings – a case of building response to a long distance earthquake." *J. Earthquake Engrg. Struct. Dyn.* 1995; 24: 1343-1353.
2. Pan, TC, Megawati K, Brownjohn JMW, Lee CL. "The Bengkulu, southern Sumatra, earthquake of 4 June 2000 (Mw = 7.7): Another warning to remote metropolitan areas." *Seismological Research Letters* 2001; 72(2): 171 – 185
3. British Standards Institution. "BS8110, Part 1: British Standard: structural use of concrete: code of practice for design and construction." 1987
4. Megawati K, Pan TC. "Prediction of the maximum credible ground motion in Singapore due to a great Sumatran subduction earthquake: the worst-case scenario." *J. Earthquake Engrg. Struct. Dyn* 2002; 31: 1501-1523
5. Megawati K, Pan TC, Kazuki Koketsu. "Response spectral attenuation relationships for Singapore and the Malay Peninsula due to distant Sumatran fault earthquakes." *J. Earthquake Engrg. Struct. Dyn.* 2003; 32: 2241-2265

6. Pan TC, Megawati K. "Estimation of peak ground accelerations of the Malay Peninsula due to distant Sumatra earthquakes." *Bull. Seis. Soc. America* 2002; 92: 1082-1094
7. Pan TC, Lee CL. "Site response in Singapore to long-distance Sumatra earthquakes." *Earthquake Spectra* 2002; 18(2): 347-367
8. Tregoning P, Brunner FK, Bock Y, Puntodewo SSO, McCaffrey R, Genrich JF, Calais E, Rais J, Subarya C. "First Geodetic measurement of convergence across the Java Trench." *Geophysical Research Letters* 1994; 21: 2135-2138
9. Zachariasen J, Sieh K, Taylor FW, Edwards RL, Hantoro WS. "Submergence and uplifte associated with the giant 1833 Sumatran subduction earthquake: evidence from coral microatolls." *Journal of Geophysical Research* 1999; 104: 895-919
10. Sieh K, Natawidjaja D. "Neotectonics of the Sumatran fault, Indonesia." *Journal of Geophysical Research* 2000; 105: 28295-28326
11. Pitts J. "A review of geology and engineering geology in Singapore." *Q. J. eng. Geol. London* 1984; 17: 93-101
12. Kohketsu K. "The extended reflectivity method for near-field seismograms." *Journal of Physics of the Earth* 1985; 33: 121-131
13. Tan SB, Lee KW. "Engineering geology of the marine member of the Kallang Formation in Singapore." *Proceedings of International Symposium on Soft Clay*, Bangkok 1977; 75-88
14. Lee KW, Zhao J, Choa V, Tan SL, Veijayaratnam M. "Geophysical investigations for assessing the construction of underground spaces in the Bukit Timah granite in Singapore." *Eleventh Southeast Asian Geotechnical Conference*, Singapore 1993; 801-806
15. Vucetic M, Dobry R. "Effects of soil plasticity on cyclic response." *J. Geotech. Engrg.* 1991; 117(1): 89-107
16. Seed HB, Wong RT, Idriss LM, Tokimatsu K. "Moduli and damping factors for dynamic analysis of cohesionless soils." *J. Geotech. Engrg.* 1986; 112(11): 1016-1032
17. Bardet, JP, Ichii K, Lin CH. "EERA – A computer program for equivalent-linear earthquake site response analyses of layered soil deposits." Department of Civil Engineering, University of Southern California, CA 2000.
18. ACI Committee 318. "Building code requirements for structural concrete and commentary." 2002.
19. Thomas W, Corinne L, Kaspar P. "The Adana-Ceyhan earthquake of June 27, 1998." The Swiss Society of Earthquake Engineering and Structural Dynamics 1998.
20. Pan TC, You XT. "Seismic response of building structures with flexible diaphragms." Civil Engineering Research, Nanyang Technological University 2004 (In Press)